Investigation of Intrinsic Stress and Transport Properties of Fe/P-Si (001) Schottky Heterojunction

Anirban Sarkar[1,2,*], S. Bhaumik[1], R. Adhikari[1,2] and A. K. Das[1]

[1]Department of Physics & Meteorology, Indian Institute of Technology, Kharagpur, India

[2]Institut für Halbleiter- und Festkörperphysik Altenbergerstr. 69, A-4040 Linz, Austria

Abstract: We present a comprehensive study on the growth morphology, the electrical and magnetic transport properties of thin iron (Fe) film on p-Si(100) substrate. The structural analysis revealed the growth of an amorphous Fe film, with low crystalline ordering and granular structure. The resistivity of the film was observed to deviate from the usual metallic behavior at lower temperature revealing a tunneling type conductance. This was also reflected in the magnetoresistance measurement of the film. The film show high positive (negative) magnetoresistance at all temperatures (below 10 K) on application of out-of-plane (in-plane) magnetic field. The current-voltage (I-V) measurement of Fe/p-Si Schottky heterojunction exhibits good rectifying property. The ideality factor (n) and Schottky barrier height (ϕ_b) of the device, at room temperature, were obtained from fitting the I-V curves. The carrier concentration of the semiconductor substrate was evaluated from the capacitance-voltage (C-V) measurements. From the measurements large deviation from the ideal value of the diode parameters was observed. All the results thus obtained show a strong correlation between the stress and the transport measurements.

Keywords: Intrinsic stress, Magnetoresistance, Schottky diode.

1. INTRODUCTION

Research in ferromagnetic (FM)/ semiconductor (SC) heterostructures has always been in limelight since they exhibit novel and interesting physical effects with technologically important applications like magnetic recording media, devices, sensors and spintronics [1]. One of the most interesting systems in this field is the Fe/Si Schottky heterojunction. Owing to the high Curie temperature and well known magnetic properties thin films of Fe prove to be great candidate as soft magnetic single layers as well as multilayers for spin based devices forming the basis of new hybrid device structures. [2-4] With the advent of the modern deposition techniques preparation of epitaxial Fe/Si heterostructure has been at a great ease, however nevertheless of the deposition technique thin films during their course of deposition develop large intrinsic stresses [5]. Frequently, these stresses are responsible for malfunction of even failure of technologically important thin film devices. The structural and growth mode correlation with magnetic and electrical properties strongly influences the device performance. Experiments have been demonstrated that surface induces an in-plane uniaxial magnetic anisotropy in variety of magnetic films grown on SC substrate. [6] As the thickness of layer is reduced, their properties are expected to be strongly influenced by surface and interfaces, which are inevitably rough at atomic scales.

The study on the evaluation of the interfacial forces in such heterostructure system is therefore important not only to know the growth morphology but also to explain various physical and transport properties. In this report, we present a systematic study on the real time stress developed due to the deposition of a ferromagnetic (FM) iron (Fe) thin film on a semiconductor (SC) silicon [*p* type Si(100)] substrate. The films are polycrystalline in nature thereby making them closer to practical devices which invariably use polycrystalline materials. The electrical resistivity and the magneto resistive properties of the thin film have been studied as a function of temperature (T) and magnetic field (H). Consequently we also present the electrical transport property of the Fe/p-Si Schottky junction, using a top-down configuration. The diode parameters were evaluated from the current-voltage (I-V) and capacitance-voltage (C-V) characteristics. The study reveals that the transport properties of the film as well as the heterojunction device have strong relation to the morphology of the thin film.

2. EXPERIMENTAL DETAILS

Two different types of *p*-type Si (100) wafers was used - (a) area 22x5 mm^2 and thickness 130 μm (for intrinsic stress, magnetization and magnetostriction measurement) and (b) area 125 mm^2 and thickness 500 μm (for the study of transport properties) having doping concentration of 7.3×10^{15} cm^{-3}. The wafers were initially cleaned ultrasonically with trichloro-ethylene (TCE), acetone and de-ionized (DI) water and etched in

*Address correspondence to this author at the Abteilung fur Festkorperphysik, Johannes Kepler University, Altenbergerstr. 69, A-4040 Linz, Tel: +43-(0)732-2468-9653; Fax: +43-(0)732-2468-9696; Email: anirban.sarkar@jku.at

E-ISSN: 2408-977X/14

hydrofluoric acid (HF) solution for 5 min. It was then rinsed in DI water, oxidized in 1:1 solution of H_2O_2:H_2SO_4 for 5 min and finally etched in HF (1:10) solution before loading into a high vacuum chamber. Fe film of thickness 120 nm prepared using electron beam evaporation at room temperature and a pressure of 2×10^{-6} mbar. A variable angle stokes ellipsometer (Model: L116S, Gaertner Scientific Corp., Chicago) was used to determine the film thickness. The X-ray diffraction (XRD) measurements were done using a X'PERT PRO MRD (PANalytical) diffractometer with Cu K_α (λ= 1.5418 Å) and the surface image of the Fe film was recorded using an Atomic Force Microscope (AFM).

We use an in-house built cantilever beam magnetometer (CBM) [7] to study the evaluation of the film strain during its growth on the SC substrate. After the deposition of film of desired thickness, the CBM device consisting of the film/substrate (Fe/Si) bi-morph system was transferred *in-situ* into two mutually perpendicular magnetic field, for the magnetic measurements (magnetization and magnetostriction). A CBM works on a simple cantilever beam principle [8-11], where the thin substrate (in the form of a rectangular plate) is clamped at one end and free at the other, thereby acting as the cantilever beam or plate. Thin films of desired materials are deposited on one side of the plate. Now do to surface adhesion between the film and the substrate any change in the dimension of the film, as a result of strain (intrinsic or magnetostrictive), would be accompanied with the displacement of the free end of the cantilever substrate from its mean position. By accurate measurement of this deflection at the free end (Δ) and equating with the bending moment of the substrate, quantitative values of the film stress (intrinsic and magnetostrictive) and magnetization can be evaluated. Experimentally Δ, is measured using lock-in-assisted differential capacitance technique details of which could be found in Ref. 10. Using simple algebraic expressions one can easily derive a relation between Δ and parameters such as, the intrinsic stress (σ_f), linear magnetostrictive constant (λ_l) and magnetization (M), respectively [10,12]. They are given as–

$$\sigma_f = -\frac{Y_s}{3(1-\nu_s)}.\frac{t_s^2}{t_f}.\frac{\Delta}{l_f\left(l_f+2l_{C/2}\right)} \tag{1.a}$$

$$\lambda_l = -\frac{2}{9}\frac{t_s^2}{t_f}\frac{Y_s(1+\nu_f)}{Y_f(1+\nu_s)}\frac{\Delta}{l_f\left(l_f+2l_{C/2}\right)} \tag{1.b}$$

$$M = \frac{Y_s w t_s^3}{6V_f H_{defl}}.\frac{\Delta}{l_f\left(l_f+2l_{C/2}\right)} \tag{1.c}$$

where the subscripts "*s*" and "*f*" represent the parameters for the substrate and the film, respectively. E,ν , *t, l, w* and H_{defl} represent the Young's modulus, Poisson's ratio, thickness, length, width and constant deflecting (or torque) field, respectively. It should be noted that, $l_{C/2}$ is the half of the length of the cantilever substrate inside the capacitor plates (where the average measurement point is considered). Following Ref. 10 and 12, Eqs. 1(a-c) has been derived considering the $t_f \ll t_s$. For the present study we use the following known typical standr values for the Fe/Si bi-morph system: $E_s = 1.85\times10^{11}$ N/m^2; $E_f = 2.11\times10^{11}$ N/m^2; t_f = 120 nm; t_s = 130 μm; l_f = 18 mm; l_s = 25 mm, ν_s = 0.28 and ν_f = 0.29.

After the CBM measurement the Fe/p-Si (500 μm) substrate was taken out for the XRD and AFM measurements and thereafter the metallization was done for ex-situ measurements. Using conventional linear four probe technique the electrical and magnetic transport properties of the Fe film as a function of applied bias (voltage), magnetic field (H) and temperature (T) was measured. Electrical contacts were prepared by evaporating Al metal with diameter 2 mm and separated by 1 mm on top of the Fe film. Keithley make 2400 source meter, 6220 current source, 2182A nanovoltmeter and 6514 system electrometer were used for the electrical measurements. For low temperature measurements closed chamber of He cryostat (Make: Cryo Industries Inc., USA) was used along with Bruker BIOSPIN electromagnet for application of magnetic field.

3. RESULTS AND DISCUSSION

3.1. Structural Charecterizations

The x-ray diffraction (XRD) pattern of the as-deposited Fe film is shown in Figure **1**, affirming a disordered amorphous system with very low order crystalline *fcc* phases. Low intensity peaks originating from the short range ordering around 2θ = 44.73^0, 55.54^0 and 65.09^0 are identified as the (110), (111) and (200) planes of the *fcc*-Fe phase, respectively. However, the (111) and (200) peak are of very low intensity and basically superimposed on an amorphous background. Absence of any other peak refers to the formation of no secondary phase, *e.g*. iron oxides or silicides. However, it must be noted that the film grown is neither epitaxial nor single crystalline. The surface morphology, as revealed by the 1μm × 1μm AFM image of the surface of Fe film (inset in Figure **1**), shows a granular structure with the grains elongated in the direction perpendicular to the incidence plane. The surface roughness and the grain size were measured to be (2.6±0.05) nm and (40±5) nm, respectively from the AFM image. Thus from the structural analysis it is observed that the Fe film has an admixture of disordered amorphous as well as low ordered polycrystalline *fcc* phases.

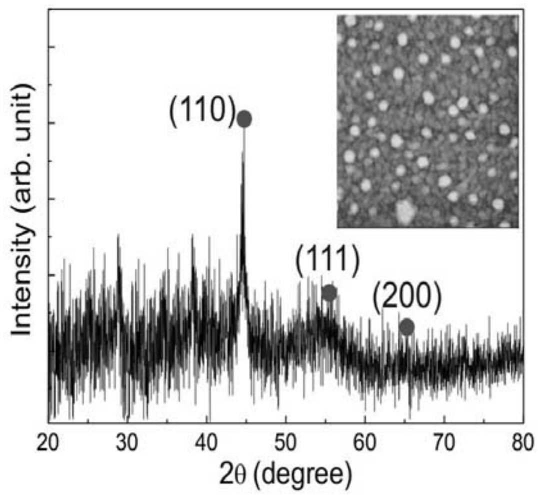

Figure 1: XRD measurement of Fe film (120 nm). The inset shows 1μm×1μm AFM image of the surface of the Fe film.

3.2. Intrinsic Stress Measurement

Figure **2** shows the variation of intrinsic stresses in terms of film force (F) normalized to width (*w*) of the Fe film deposited onto the Si(100) substrate at room temperature. It is to be noted that the film force depends linearly on the thickness (*t*) for constant stress ($F/w = \sigma t$). Thus the value of the intrinsic stress developed in the film could be easily evaluated from the slope of the stress-thickness versus thickness curve. The plot is divided into three distinct regions. At the start of each experiment, keeping the shutter of the evaporator closed (*i.e*., no deposition is taking place), the system is stabilized initially for few seconds (region 1). Then the shutter is opened (*i.e*., deposition is taking place) and the measured data are represented by region 2. At the end of the experiment the shutter is again closed (*i.e*., no deposition is taking place) and data collection is continued in this state for few more seconds (region 3). The force curve in Figure **2** depicts a Volmer-Weber type growth, which is primarily observed in polycrystalline thin film. It is well known that the Volmer-Weber growth mode comprises three different growth stages: (a) the precoalescence stage, where isolated islands nucleate and grow, (b) the coalescence stage, where islands merge and percolate and the remaining channels are filled, and (c) followed by the growth of continuum film thereon.

During the initial stage of deposition a compressive stress is observed in the thickness range of 0.55±0.02 nm, which corresponds to almost 4 monolayers (ML) of Fe film (see inset of Figure **2**). Due to the capillarity effect (surface tension) the lattice parameter of isolated metal particles is expected to be smaller than that of the respective bulk phase. As the particle nucleates and grows to form isolated islands, their equilibrium lattice parameter increases and gradually tries to approach the respective bulk value. However, this is inhibited as the particles are anchored to the substrate by adhesion. This develops a compressive strain within the particle due to restriction (since adhesion with the substrate) in expansion of crystal lattice upon particle growth, identified by the initial dip at the start of deposition.

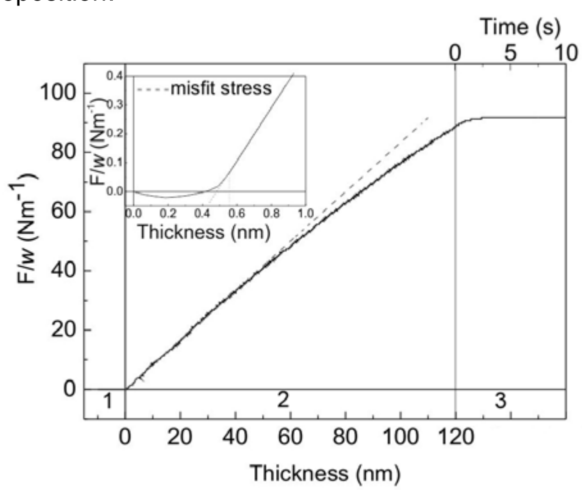

Figure 2: Force per unit film width F/*w* evolving as a function of mean film thickness and time during and after the growth of Fe on the Si substrate; the inset shows the zoomed image of the force curve at lower thickness. The dashed line represents the constant strain in the film during initial stage of the film growth.

Due to subsequent growth, the isolated islands grow and majority of the lattice expansion strain is continuously relaxed because of the weak film/substrate adhesion which is not strong enough to withstand the compressive stress. As the surface free energies of the isolated islands are greater than the free energy of the grain boundary, if created by coalescence, [13-15] the islands are snapped together (zipping effect) and generate a tensile stress within the continuous network of the islands because of forming the grain boundaries (GB). This can also be observed in the nature of the force curve, where with the increase in the film thickness the force switches from compressive to tensile reaching a constant value of 0.84±0.05 GPa (shown by the dashed lines in Figure **2.** In disordered polycrystalline film the grain boundaries acts as an atomic sink and have reduced atomic density. The behavior of the stress during growth of the film after crystallite coalescence depends greatly on the mobility of the deposited atoms. For Fe, which has low adatom mobility (*e.g.*, Fe), the rate of diffusion on the surface of the growing film is low compared to their rate of arrival from the vapour. As a consequence further growth takes place over a strained system resulting in continuous growth of the tensile stress. At higher thickness (> 60nm) the slope of the force curve decreases because part of the strain is relieved by the formation of defects such as, dislocations and/or grain boundaries. When the deposition is stopped the tensile stress tends to saturate; little variation of the stress at the end of deposition is due to recrystallization process which tend to relax the developed tensile stress.

Considering the bulk lattice constants of Fe ($2a_f$ = 0.5733 nm) and Si (a_0 = 0.5431 nm) the lattice misfit $[(a_0 - a_f) / a_f]$ equals 5.27% corresponding to a compressive misfit strain of 11 GPa. This value is much larger that the experimentally obtained value of the stress. The reason being that, the Fe film does not grow epitaxially and is disordered (with low polycrystalline ordering) in nature. Granular film is obtained with large defects and grain boundaries. As a result, due to the formation of such grain boundaries and misfit dislocations, the strain is relaxed over the whole thickness of the film. It should also be noted that at elevated substrate temperature and larger thickness (>130 nm) where the defects are neutralized the film forces can switch to compressive in accordance with the maximum misfit strain.

Similar to the structural analysis the stress curve also reveals the growth of a disordered Fe film. From the result thus obtained we could also infer that the Fe film thus deposited on the silicon substrate is (a) granular in nature, (b) highly strained at the semiconductor interface, (c) consisting of large defects and grain boundaries, and (d) the growth takes place via columnar type Volmer-Weber mode.

3.3. Magnetization and Magnetostriction Measurements

Figure **3(a)** shows the room temperature variation of the Fe film magnetization (M) as a function of externally applied magnetic field (H). The hysteresis loop is obtained by varying the magnetizing field (H_m) in a closed loop and measuring the substrate deflection in a deflecting magnetic field (H_{defl}) of 10 mT. It is observed that the saturation magnetizations of Fe films 1.21 ± 0.02 MA/m (coercivity: H_C = 10 mT), is in good agreement with the reported values in literature [16]. However, the saturation magnetization lies significantly below the bulk value probably due to considerable reduction in dimension and structural disordering in the film, as revealed from the XRD and AFM results, which in turn destroys long range magnetic ordering in the film.

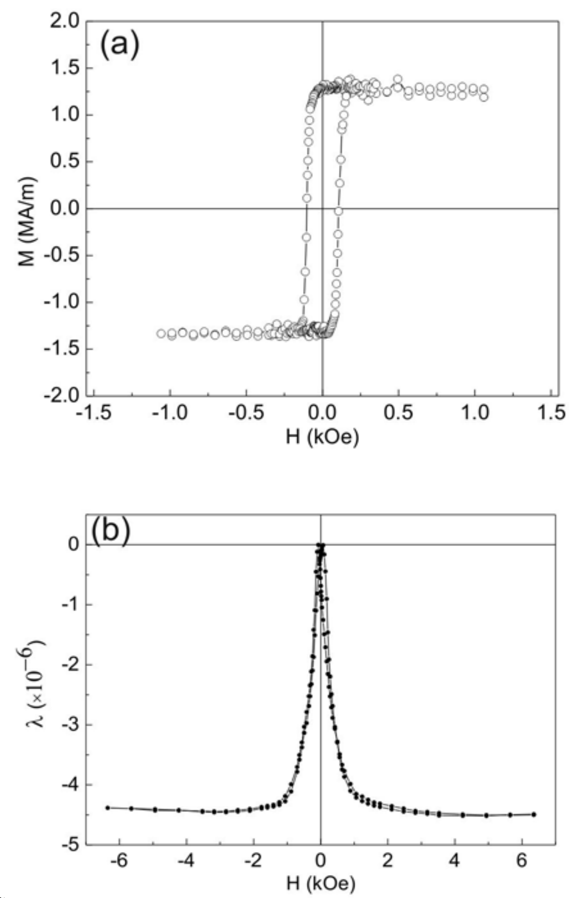

Figure 3: (a) Magnetization as a function of applied field at room temperature for Fe film; and **(b)** variation of linear magnetostriction with field applied along the length of the film, measured at room temperature.

The magnetostrictive property of the Fe/p-Si bimorph system is shown by the curve in Figure **3(b).** The magnetostriction constant (λ) is measured from the substrate deflection by applying the saturation magnetic field to the bi-morph along its length, the experimental saturation value therefore corresponds to the saturation magnetostriction λ_s. From the curve the value of λ_s is obtained to be equal to -4.5×10^{-6} and is in good agreement with the corresponding bulk value.

Quantitative value of the polycrystalline magnetoelastic coupling constant B can also be estimated using the relation,

$$\lambda_s\left(\frac{Y_f}{1-\nu_f}\right)=-\frac{2}{3}B. \qquad (2)$$

It should be noted that λ_s and B both are independent of the film thickness. Using Eq. (2), we obtain B_{Fe} = 1.104 x 10^7 erg/c.c for the Fe-film, in study. Similar results were obtained for magnetic field in direction perpendicular to the plane of the film due to magnetically isotropic nature of the prepared film.

3.4. Transport Properties of the Ferromagnetic Film

Figure **4** shows the temperature dependence of the zero-field resistivity of the Fe film. At higher temperature the *ln* ρ shows a T^2 dependence attributed to the phonon mediated scattering characteristics of the metallic film. However, below 100 K the resistivity shows a typical non quadratic dependence on the temperature, $\ln\rho \propto T^{\alpha}$ (where α = 0.57), which is the characteristics of tunneling conduction across the grain boundaries between the localized conduction states [17]. Some order of non-linearity in the resistivity profile of the film is still observed, which might be due to the presence of surface oxide layers. It is observed from the structural and stress measurements that the Fe-film is granular in nature and isolated islands (composed of the Fe granules) are dispersed over the film surface.

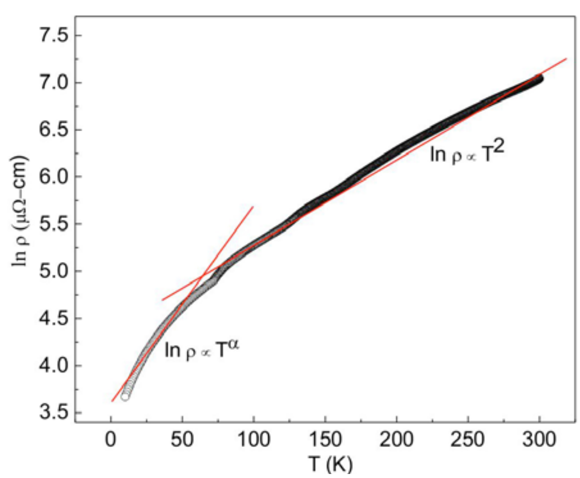

Figure 4: Variation of resistivity with temperature of the Fe-film.

Thus at higher temperature the carriers has sufficient thermal energy to cross across the potential barrier of the grain boundaries, however, at lower temperature the electrical conductance is expected to be dominated by tunneling mechanism through the grain boundaries among the weakly localized sites of the Fe-granules.

Figure **5(a)** and **(b)** shows the variation of the magnetoresistance $\left[MR=\left(R(H)-R(0)\right)/R(0)\right]$ of the Fe film at different temperatures, on application of magnetic field (H) in direction out-of-plane and in-plane, respectively, to the in-plane applied current. From the results it is observed that: (a) the MR is positive at all temperatures on application of out-of plane field; (b) under in-plane field MR is positive

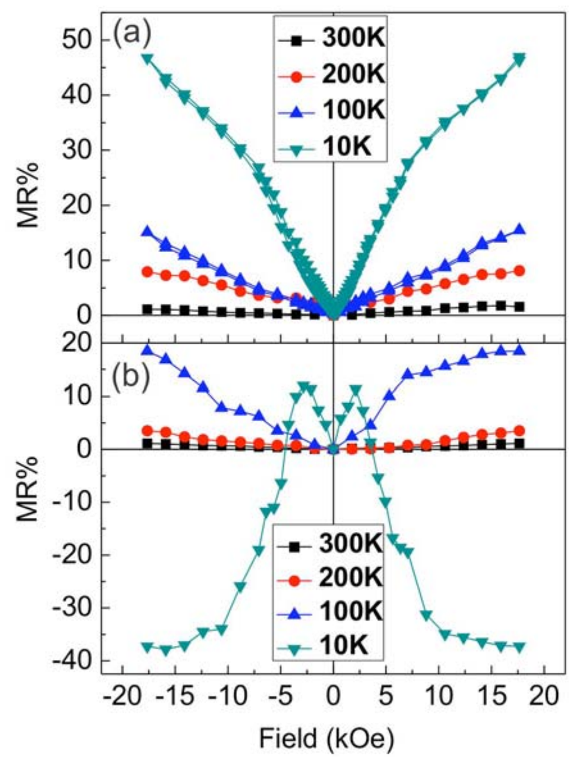

Figure 5: Magnetoresistance (MR) of Fe-film measured on application of field (H), (a) perpendicular and (b) parallel, to the direction of current as well as the plane of the film.

above 100 K and negative below it; (c) in all cases, at H = 0 the MR profile is almost symmetric; and (d) the MR value is positive and much larger than that normally observed for FM polycrystalline metal films where one expects negative MR. As revealed earlier from the structural analysis that the film is a highly disordered granular system with weakly localized magnetic states. This could result in large spin fluctuations on application of magnetic field thereby resulting in large positive MR (PMR) in the system, as suggested in the literature [18, 19]. The film being magnetically isotropic, the MR is invariable under the change of the magnetic field direction (in or out-of plane). However, the thickness of the film being less compared to film/substrate system, the motion of the electron is limited in the case of in-plane H, resulting in a lower magnitude of MR as compared to the out-of plane H. At sufficient low temperature T < 100 K, the transport is dominated by the tunneling mechanism across grain boundaries via localized grain (as suggested from the resistivity profile) resulting in low spin-flip scattering. Application of in-plane H, under such condition induces tunneling of electrons among magnetically aligned grains. This result in further suppression of the "spin-flip" or "spin-exchange" scattering at the strained grain boundaries, thereby decreasing the MR. At low field, maximum antiparallel alignment of the magnetization of alternating grains/ domains within the granular system results in the slight increase in the magnitude of MR.

Alternatively, the large PMR could be explained by considering a spin dependent layer formed at the vicinity of the FM/SC junction. We anticipate that the p-Si, although, being highly resistive $\left(\rho_{Si} >> \rho_{Fe}\right)$ has some influence in on the magnetoresistance effect. We take account of the following assumptions: (i) thin native oxide layer (~ 1 nm) of SiO_2 lies at the interface between the Fe-film and Si surface, (ii) spin polarized carrier tunnels through the oxide layer and enters the SC creating a spin accumulation layer near the interface by overcoming the FM/SC Schottky energy barrier, (iii) the spin accumulation layer has a magnetic moment with orientation determined by the domain structure of the Fe film, and (iv) thermal vibration at higher temperature destroys the magnetic ordering of the accumulation layer. A schematic representation of the magnetic layer formed inside the SC is shown in Figure **6.** At low temperature (10 K) an anomalous behavior of the MR characteristics is observed for the Fe film. The FM/SC heterostructure now acts like a GMR element, with two magnetic layers (Fe film and the accumulation layer) separated by an insulating layer (native oxide layer) with the measurement done in a current-in-plane (CIP) mode. Under application of in-plane H, the magnetization direction in both layers orients parallel to each other (as shown in Figure **6(a)**). These results in low spin dependent scattering in the system and rendering a negative contribution to the total MR. On the other hand, the polarized spins entering into the SC starts to precess within the SC (as shown in Figure **6(b)** on application of H in out-of-plane direction. Thus the resistivity increases because of greater spin flip scattering is induced in the SC accumulation region.

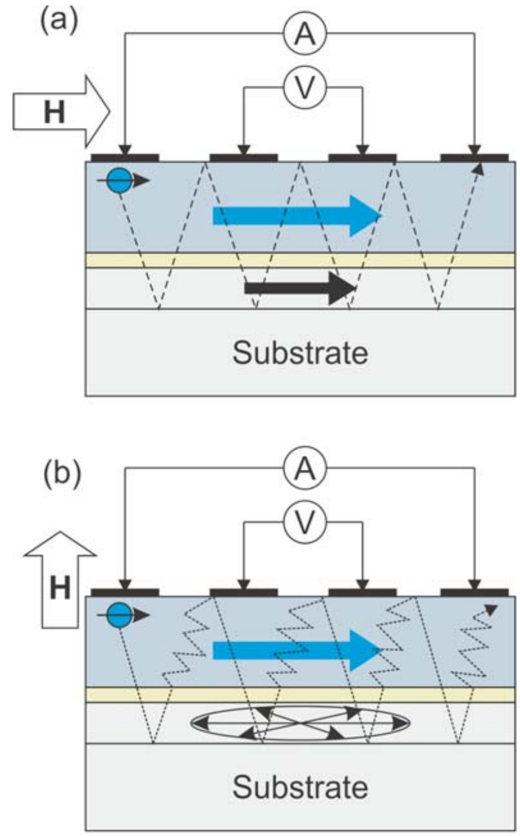

Figure 6: Schematic representation of the CIP mode of the measurement of magnetoresistance of the Fe film with magnetic field applied (a) in-plane and (b) out of plane, to the film.

3.5. Devicee Characteristics of FM/SC Heterostructure

Figure **7** shows the room temperature I-V charateristics of the Fe/*p*-Si Schottky device; the inset of Figure **7** shows the respective semi-log plot. The device shows good rectifying property with very

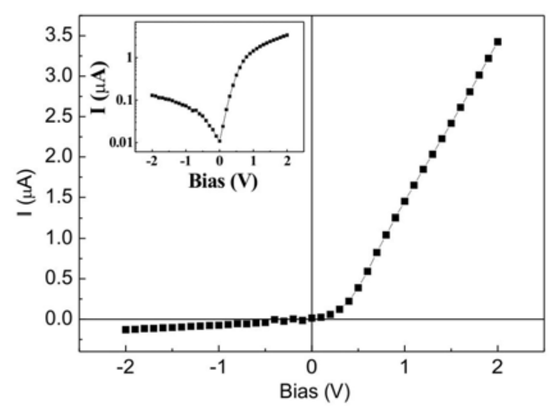

Figure 7: Current (I)-voltage (V) characteristics of Fe/p-Si, measured at 300 K. In the inset shows the semilog I-V characteristics representing the Schottky behavior.

negligible current flowing under reverse bias. Using the thermionic emission (TE) theory [20], the ideality factor (*n*) and the barrier height (ϕ_b) can be obtained from the slope and current axis intercept of the linear region of the forward bias I-V characteristics, respectively. The values of ϕ_b and *n* was evaluated to be 0.84 eV and 5.9. The downward curvature of the forward bias log I-V plot (as seen in the inset of Figure **7**) is caused by the effect of the series resistance (R_s). The R_s values have been calculated using the method developed by Cheung and Cheung [21]. According to Cheung et. al. the forward bias I-V relation of the Schottky diode with series resistance can be expressed as,

$$I = I_0 \exp\left[q\left(\frac{V - IR_s}{nkT}\right)\right], \tag{3}$$

where IR_S term is the voltage drop across the series resistance (R_S) of the device, *q* is the electronic charge, *k* is the Boltzmann's constant and T is the absolute temperature. The reverse saturation current I_0 is given by –

$$I_0 = AA^*T^2 \exp\left[-\frac{q\phi_b}{kT}\right] \tag{4}$$

Thus from eqn. (3) and (4) one can write,

$$V = \left(\frac{nkT}{q}\right)\ln\left(\frac{I}{AA^*T^2}\right) + IR_s + n\phi_b \tag{5}$$

Let us define a term dependent on the current of the device as,

$$P(I) = n\phi_b + IR_s \tag{6}$$

Thus from eqn.(5), $P(I) = V - \left(\frac{nkT}{q}\right)\ln\left(\frac{I}{AA^*T^2}\right)$ (7)

The value of R_s can thus be determined from the derivative of eqn. (5),

$$\frac{dV}{d(\ln I)} = \frac{nkT}{q} + IR_s, \tag{8}$$

A plot of *dV*/*d*(ln *I*) versus *I* will be linear and gives R_s as the slope and nkT/q as the y axis intercept from eqn. (6). Figure **8** shows the plot of *dV*/*d*(ln *I*) versus *I* at room temperature. The value of n and R_s has been calculated as 13.1 and 2664 Ω, respectively. It is observed that large difference between the value of n obtained from the forward bias *ln*I-V plot and that obtained from P(I)-I curve. This may be attributed to the existence of the series resistance and interface states and to the voltage drop across the interfacial layer. Also it should be noted that in the earlier case the functions were extracted from the linear region of the I-V plot while Cheung functions are only applied to the non-linear region in the high voltage section of the forward bias lnI vs V curve.

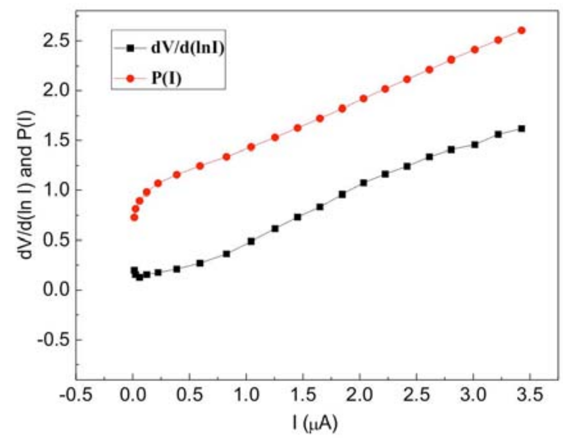

Figure 8: dV/d(lnI) and P(I) versus I plot of the Fe/p-Si heterojunction.

A quantitative idea about the carrier concentration (N_A) of the SC, the diffusion potential (V_d) and barrier height (ϕ_b) of the Schottky junction could be evaluated from the capacitance (C) – voltage (V) characteristics of the heterostructure. There are basically two types of capacitance associated with a *p-n* junction: (a) the *junction capacitance* due to dipole in the transition region, which is dominant under reverse bias condition; and (b) the *diffusion capacitance* due to the charge storage effect, which is dominant when the junction is forward bias. For metal/SC Schottky diode, measurements of the C–V can provide knowledge about the fixed charge carrier concentration and the barrier height. Figure **9** shows C^{-2}-V characteristics of Fe/p-Si. From the Mott-Schottky [20] relationship between capacitance and voltage,

$$\frac{1}{C^2} = \frac{2}{qN_A\varepsilon_0\varepsilon_r A^2}\left(V_d - V\right). \tag{9}$$

Where, ε_0 = dielectric constant of free space, ε_r = dielectric constant of the semiconductor material, N_A = acceptor doping density and V_d = the built-in potential or the diffusion potential. The Schottky barrier can be evaluated from the relation,

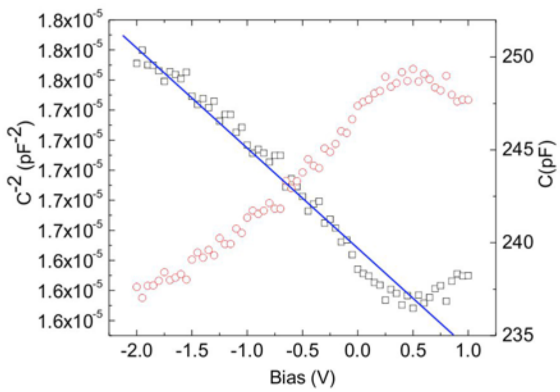

Figure 9: Capacitance (C)-Voltage (V) characteristics of the Fe/p-Si heterojunction**.**

$$\phi_b = eV_d + x, \tag{10}$$

where x (= 0.28 eV) is the energy difference between the bulk Fermi level and the valance band. From the slope of the linear region of the C^{-2}-V characteristics acceptor doping concentration was calculated to be 7.3×10^{15} cm^3. From the intercept and eqn. (10) the diffusion potential (V_d) and the barrier height is estimated as 0.68 eV and 0.96 eV, respectively. A small discrepancy in the value of ϕ_b obtained from the I-V and C-V characteristics are because the former accounts for the detailed distribution of carriers at the interface while the latter averages over the whole area.

Nevertheless, the value of ϕ_b is higher than that observed normally this could be explained by the existence of the interfacial layer and trap states in the SC. As we know from the stress measurements, relaxation of the misfit strain in the system could also be obtained by interdiffufion across the FM/SC interface. Such large interdiffusion between the Fe and Si at the interface could also result in higher values of the barrier height. Even the obtained values of the ideality factor are much higher than from ideal metal/SC Schottky junction diode. Such high value of *n* are attributed to secondary mechanism, which includes interface dipoles due to interface doping or specific interface structure, as well as fabrication induced defects. As a result, other modes of carrier transport might dominate over the thermionic emission of charge carriers, for example, image force lowering, the generation-recombination current, current due to injection of minority carriers into the SC and tunneling across the oxide interface. Also the lateral barrier inhomogenety across the FM/SC interface often produces a wide distribution of low-Schottky barrier patches which again results in such increase in the value of *n*. As observed from the stress measurements, owing to the large stress induced in the granular Fe film, such inhomogenety is normally expected.

4. CONCLUSIONS

It is very important not only scientifically but also technologically to know the correlations among various physical properties with the morphology of thin films. In the same vein, we have studied the growth morphology of thin Fe film deposited on p-Si substrate, and observed that it has a strong influence in determining the magnetic and transport properties of the system. High tensile stress is developed as the Fe-film is deposited on the Si substrate at room temperature, however the magnitude of the strain within the system is lower that the lattice misfit strain indicating large relaxation processes by formation of grain boundaries, recrystallization, defects, interdiffusion and so on. This results in highly defect states and disordered/non-uniform barrier across the FM/SC interface. The stress measurement also reveals that the film growth takes place via Volmer-Weber mode and is granular in nature. Using a simple cantilever technique we determine the magnetization and the magnetostriction coefficient of the Fe film. Both the saturation values were observed to be below the bulk values attributed to the low dimensionality of the granular film as well as the amorphous phases in the system. This reveals that the structural ordering of the Fe film has a great influence in determining the magnetic property of the Fe-film.

Supporting the stress measurement the XRD and AFM results also shows a disordered amorphous phase of Fe film, with very low crystalline ordering of the *fcc*-Fe phase. Due to such disordered system the resistivity at low temperature deviates from normal metallic behavior and a tunneling type conductance is observed. Also the granular nature of the film attributes to the observance of an anomalous positive magnetoresistance at higher temperature. As at low temperature, the conduction is dominated by tunneling mechanism via localized grains and due to application of magnetic field resulting in sufficient decrease in the magnetoresistance.

Finally, the I-V and C-V measurement of the Fe/p-Si heterojunction Schottky device was done to study the transport characteristics across the junction.

Quantitative values of the ideality factor, barrier height, series resistance, the diffusion potential and the carrier concentration was obtained. Interestingly, the study of the film as well as the Schottky device is observed to be profoundly affected by the nature of growth and the amount of defects/ interface states present. The study of intrinsic stress measurement thus provides a platform for better understanding of the morphology of the device and its transport properties. The results thus obtained shows that the electrical as well as the magnetotransport properties of the thin films has strong co-relation to the morphology of the film. Moreover, due to its large magnetoresistance and magnetostrictive effect, such FM/SC bi-layer system promises their use as magnetic field sensors.

ACKNOWLEDGEMENTS

We would like to acknowledge the financial support of Council of Scientific and Industrial Research, Govt. of India, for providing the financial support to peruse the work. We would also like to thank Prof. S. K Roy from the Department of Physics and Meteorology, IIT Kharagpur, for the C-V measurements.

REFERENCES

[1] Žutic I, Fabian J, and Sarma SD. Rev. Mod. Phys.2004; 76: 323.

[2] Hanbicki AT, Van 't Erve OMJ, Magno R, KioseogloucG, Li CH, Jonker BT, Itskos G, Mallory R, Yasar M, and Petrou A. Appl. Phys. Lett. 2003; 82: 4092.

[3] Hall KC and Flatté ME. Appl. Phys. Lett. 2006; 88: 162503.

[4] Zhu HJ, Ramsteiner M, Kostial H, Wassermeier M, Schönherr HP, and Ploog KH. Phys. Rev. Lett. 2001; 87: 016601.

[5] Klokholm E, and Berry BS. J. Electrochem. Soc. 1938; 118: 823.

[6] Wulfhekel W, Knappmann S and Oepen HP. J. Appl. Phys. 1996; 79: 988.

[7] Sarkar A, Adhikari R, and Das AK. Current Science 2013; 104: 826.

[8] Klockholm E. Rev. Sci. Instru. 1969; 40: 1054.

[9] Sander RD, Enders A, and Kirschner. J. Rev. Sci. Instru. 1995; 66: 4734.

[10] Koch R, Leonhard H, Thurner G, and Abermann R. Rev. Sci. Instru. 1990; 61: 3859.

[11] Langier M. Thin Solid Films 1981; 75: 213.

[12] du Trémolet de Lacheisserie E, and Peuzin JC. J. Magn. Magn. Mater. 1994; 136: 189.

[13] Finegan JD and Hoffman RW. J. Appl. Phys. 1959; 30: 587.

[14] Hoffman RW, in Physics of Thin Films, edited by G. Haas and R. E. Thun (Academic Press, New York, 1966), Vol. 3.

[15] Hoffman RW. Thin Solid Films 1976; 34: 185.

[16] M. Weber, R. Koch, and K. H. Rieder. Phys. Rev. Lett. 1994; 73: 1166.

[17] Glazman LI, and Matveev KA. Sov. Phys. JETP 1988; 67: 1276.

[18] Mallik R, Sampathkumaran EV, and Paulose PL, Appl. Phys. Lett.1997; 71: 2385 and reference thereon.

[19] Peng DL, Sumiyama K, Konno TJ, Hihara T, and Yamamuro S. Phys. Rev. B 1999; 60: 2093 and reference thereon.

[20] Sze SM. Physics of Semiconductor Devices, 2nd ed. (Wiley, NY, 1981).

[21] Cheung SK, and Cheung NW, Appl. Phys. Lett. 1986; 79: 85.

Received on 16-06-2014 Accepted on 19-06-2014 Published on 28-08-2014

http://dx.doi.org/10.15379/2408-977X.2014.01.01.5